$\pi h_{11/2}$ intruder and $\pi g_{9/2}^{-1}$ strongly coupled bands in ^{115}Sb

R. S. Chakrawarthy and R. G. Pillay
Tata Institute of Fundamental Research, Bombay 400 005, India
(Received 8 November 1995)

High spin states have been populated in ^{115}Sb with the reaction ^{100}Mo(^{19}F,4n)^{115}Sb at a beam energy of 82 MeV. Two intruder rotational bands ($\Delta I=2$) extending to spins $43/2^-$ and $51/2^-$ have been observed. The extracted relative $B(E2)$ value supports the nearly diabatic nature of these two bands. The transition energies in these two bands are nearly similar and the bands have a relative spin alignment of $4\hbar$ at low frequencies. The bands have been interpreted to be based on the $\pi h_{11/2}$ orbital coupled to the deformed $2p$-$2h$ states of the ^{114}Sn core. Possible quasiparticle configurations for the excited negative parity band are discussed and it is suggested that this band is based on aligned $h_{11/2}$ neutrons, the yrare extension of which is observed diabatically down to very low spin values. Two strongly coupled ($\Delta I=1$) rotational bands involving the $(\pi g_{9/2})^{-1}$ configuration have been observed, of which the known strongly coupled band has been extended from $23/2^+$ to $37/2^+$ in spin and the extracted $B(M1;I\rightarrow I-1)/B(E2;I\rightarrow I-2)$ values for this band are compared with the Dönau-Frauendorf formula. Alignment features due to the $h_{11/2}$ neutrons in the observed bands are compared with the core nucleus ^{114}Sn and cranked shell model calculations. Equilibrium deformations for a range of odd Sb isotopes have been calculated with various intrinsic proton configurations. [S0556-2813(96)04310-5]

PACS number(s): 21.10.Re, 23.20.Lv, 27.60.+j

I. INTRODUCTION

The odd mass Sb nuclei display a variety of excitations at low to very high spins. At low spins, proton shell closure effects at $Z\sim 50$ manifest themselves in the form of vibrational and near spherical excitations [1], whereas the high spin structure is dominated by intruder rotational bands extending to $(81/2)\hbar$ [2]. The intruder bands in Sb isotopes arise due to the coupling of the odd proton to the deformed states of the Sn core. The deformed states in Sn nuclei are due to the proton two-particle-two-hole ($2p$-$2h$) excitation across the $Z=50$ shell gap, the underlying configuration being $(\pi g_{7/2})^2\otimes(\pi g_{9/2})^{-2}$ [3]. These states have prolate deformation and occur at a low excitation energy of ~ 2 MeV. Structures involving a valence proton coupled to both spherical and deformed core states have been observed in the odd mass Sb isotopes and are best exemplified in the midshell nucleus ^{117}Sb [4], in which spherical and deformed states built on the proton configurations $d_{5/2}$, $g_{7/2}$, and $h_{11/2}$ were observed. Bands with enhanced deformation due to the odd proton in $h_{11/2}$ orbital have been mapped out in a number of odd mass Sb and iodine isotopes [2,5–7]. The strongly-β-sloping π [550]$1/2^-$ intruder orbital is thought to stabilize enhanced deformation as was observed in ^{113}Sb, wherein the $\pi h_{11/2}$ intruder band was found to have a deformation value $\beta_2=0.32$ [2]. Apart from the decoupled bands both the odd-even and odd-odd Sb nuclei exhibit high-K rotational bands, characterized by little or no signature splitting, based on the $\pi g_{9/2}^{-1}$ configuration [8,9]. Recently, high spin study of intruder bands in this mass region has received an impetus following the discovery of a novel form of gradual band termination at frequencies greater than 1.0 MeV/$\hbar$. At such frequencies, the bands in ^{109}Sb [5] and ^{106,108}Sn [10,11] have dynamic moments of inertia approximately one-third the rigid body value. This has been interpreted as a smooth termination of a collective rotational band in which the spin of the valence configuration is gradually exhausted [12,13].

In the present paper we report the γ-ray spectroscopy of ^{115}Sb, in which we have observed two strongly coupled bands and two intruder-type rotational bands. One of the strongly coupled bands shows clear evidence of a sharp alignment of $h_{11/2}$ neutrons, whereas one of the intruder bands shows a delay in alignment of the $h_{11/2}$ neutrons compared to the cranked shell model calculations and the neighboring even-even nucleus ^{114}Sn [14].

II. EXPERIMENTAL PROCEDURE AND DATA ANALYSIS

The experiment was done at the 14 UD BARC-TIFR Pelletron accelerator facility, Bombay. States in ^{115}Sb were populated with the reaction ^{100}Mo(^{19}F,4n)^{115}Sb at a beam energy of 82 MeV, with a thick target of 4 mg/cm^2 ^{100}Mo backed by 10 mg/cm^2 of Au. At this beam energy the dominant channel was 4n, leading to ^{115}Sb. The other channels populated in this reaction were 3n, 5n, and $p4n$. The emitted gamma rays were detected with an array of five Compton-suppressed germanium detectors (CS-HPGe) and a 14-element NaI multiplicity filter [15]. The five CS-HPGe detectors are in a planar geometry at angles 15°, $\pm 45°$, and $\pm 75°$ with respect to the beam axis. The energy resolution of each HPGe detector was 2.0–2.2 keV at 1.33 MeV and had a relative efficiency of 25% at $E_\gamma=1.33$ MeV. The experiments involved γ-ray excitation function and γ-γ coincidence measurements. Twofold Ge events, within a time coincidence window of 200 nsec, qualified by a hardware trigger comprised of at least three NaI detectors, were collected. In all, 65×10^6 coincidences were accumulated in the list mode experiment. The individual count rate of CS-HPGe detectors was less than 10 kHz in this experiment. The efficiency and energy calibration of the HPGe detectors was taken using ^{152}Eu source and the relative efficiency of Ge

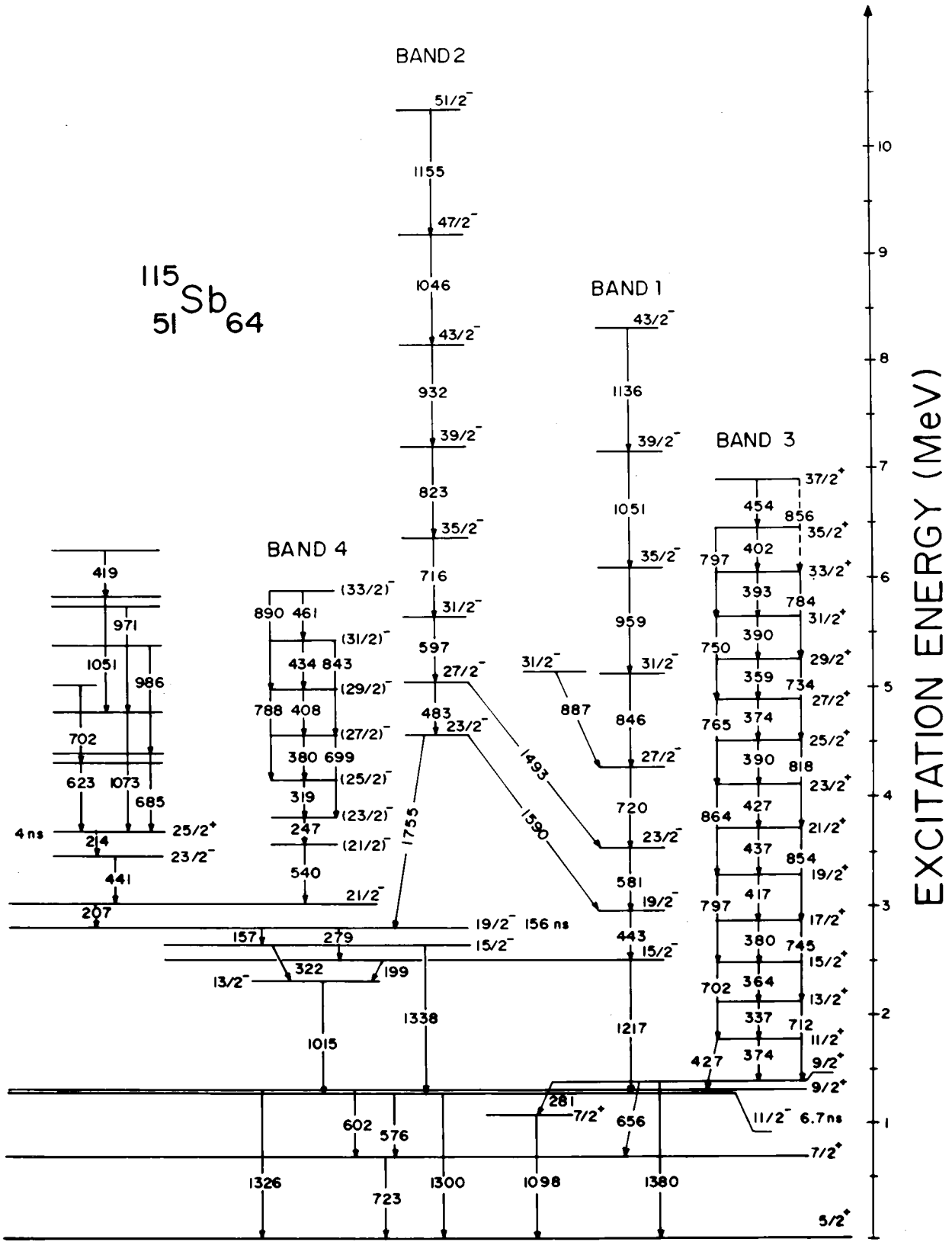

FIG. 1. The level scheme of ^{115}Sb from the present experiment. Transition energies are marked in keV.

detectors was obtained from the radioactivity background data accumulated during the experiment. In the off-line data analysis, the raw list data were recalibrated to 0.5 keV/channel. The background-subtracted singles spectra were projected from the list data and were analyzed for new transitions. Spin assignments were based on the ratios of the directional correlation ($R_{\rm dco}$), obtained from the detectors at 15° and 75°. The $R_{\rm dco}$ value, defined as

$$R_{\rm dco}=\frac{(I_{\gamma 1}\ \text{at}\ 15^\circ\ \text{gated by}\ \gamma_2\ \text{at}\ 75^\circ)}{(I_{\gamma 1}\ \text{at}\ 75^\circ\ \text{gated by}\ \gamma_2\ \text{at}\ 15^\circ)}, \quad (1)$$

was obtained by gating on quadrupole transitions. The $R_{\rm dco}$ value was close to 1.0 for a stretched $E2$ transition and close to 0.5 for a stretched dipole transition. Also, angular distributions were obtained, for a few transitions, from singles data with the detectors at angles 15°, 45°, and 75°. These intensities were corrected for the relative efficiency of the HPGe detectors and fitted to the function

$$W(\theta)=A_0+A_2P_2(\cos\theta). \quad (2)$$

A. Level scheme

The level scheme of ^{115}Sb was constructed based on coincidence relationships and relative intensities and is shown in Fig. 1. The transitions in ^{115}Sb with their intensity and spin assignments are given in Table I. The A_2 coefficients of some of the γ transitions are given in Table II. The γ-ray intensities were obtained from the total projection of γ-γ coincidence data and singles measurements for states below isomer(s) after appropriate normalization. The new features of this study are the bands 1 and 2, the extension of the known strongly coupled band 3 to higher spins, and the strongly coupled band 4. The present study extends the previously known level scheme of ^{115}Sb to an excitation energy of $\sim$10 MeV and a spin of $I^\pi=51/2^-$. The known energy levels reported in [8,16] have been observed in the present experiment and have been confirmed. The g factors of the isomeric states at $I^\pi=11/2^-$ and $19/2^-$ levels were measured using the time differential perturbed angular distribution (TDPAD) technique by Shroy *et al.*, Ketel *et al.*, and Faber *et al.* [17,18,8] with the $(p,2n)$, $(\alpha, 4n)$, and (^{6}Li, $3n$) reactions, respectively. Based on their studies the configuration of the $11/2^-$ state was suggested to be an admixture of $\pi h_{11/2}$ configuration and $\pi d_{5/2}$ configuration coupled to the 3^- state of the Sn core. The g factor of the $19/2^-$ state was deduced to be $\sim$0.29. Faber *et al.* [18] suggested that the configuration of this state is mainly a three-particle state involving the odd proton in $d_{5/2}$ orbital coupled to the 7^- state of ^{114}Sn, although Bron *et al.* [16] have inferred from the $B(E2)$ enhancement over the single-particle estimate that this state may have admixtures of $\pi h_{11/2}\otimes 4^+$ state of the Sn core.

The set of spherical levels feeding the isomeric state at $I^\pi=19/2^-$ has been extended. Several new transitions have been found to feed the spherical state at $I^\pi=25/2^+$, extending this set to 6 MeV. The work of Bron *et al.* done with the ^{113}In$(\alpha,2n)^{115}$Sb reaction have observed, in addition, the γ transitions 1213.6 and 1012.7 keV feeding the $7/2^+$ spherical state. These transitions, however, were not observed in the present experiment. This may be due to the heavy-ion-induced reaction which selectively excites high spin states.

B. Band 1

Figure 2 shows the γ-γ coincidence spectra with gates set on all the band members. The set of γ transitions at 443, 581, 720, 846, 959, 1051, and 1136 keV constitute this band. The $I^\pi=15/2^-$ state of this band depopulates through the 1217 keV γ transition. Based on lifetime information Bron *et al.* [16] and Shroy *et al.* [8] have assigned the 1300 keV γ transition, depopulating the $I^\pi=11/2^-$ state, a $M2$ multipolarity. The one at 1217 keV being an $E2$ transition, the present band beginning at $I^\pi=15/2^-$ has been assigned negative parity. Angular correlation data assign an $E2$ character to the members of this band. This band extends to $I^\pi=43/2^-$. A forking at spin $27/2^-$ has been observed and the 887 keV γ transition has $E2$ multipolarity. The ordering of 581 and 443 keV γ transitions is different from that of Shroy *et al.* [8] and our placement agrees with that of Bron *et al.* [16].

C. Band 2

Band 2 is a weak band and has been observed to feed into band 1 at $I^\pi=19/2^-$ and $23/2^-$ through the 1493 and 1590 keV γ transitions, respectively. The γ transitions at 483, 597, 716, 823, 932, 1046, and 1155 keV are members of this band. The 1755 keV γ transition depopulates the $I^\pi=23/2^-$ state of this band and feeds the known isomer at the $I^\pi=19/2^-$ state. From the angular distribution analysis we have deduced a positive A_2 value, $0.52(\pm 0.15)$ (Table II), for the 1493 keV γ transition, thereby ruling out an $E1$ transition. The $R_{\rm dco}$ value between stretched quadrupole transitions (members of band 1 and band 2) and the 1493 keV γ transition is 0.9(2). Therefore, this band has been assigned negative parity. This band becomes yrast at a spin $(43/2^-)\ \hbar$ and extends to $I^\pi=51/2^-$. Figure 3 shows the gated spectra of this band with the gates set on all the transitions of this band.

D. Band 3

The known strongly coupled band has been extended from $(23/2^+)$ to $(37/2^+)\hbar$ in spin. Apart from the known transitions through which this band deexcites, we have found a weak 281 keV transition which depopulates the energy level at $I^\pi=9/2^+$ and feeds the second $I^\pi=7/2^+$ state, this energy level was reported by Bron *et al.* [16]. There are several transitions in this band which are nearly degenerate and are seen in the self-gated projected spectra. The observation of crossover $E2$ transitions has helped to pin down their placements in the level scheme. The gated spectra of the 1326 and 1380 keV γ transitions clearly show the presence of the second 374 and 427 keV γ transitions which have been placed in the level scheme at higher spins. Figure 4 shows the spectrum with gate set on the 364 keV γ transition.

The $\Delta I=1$ mixed $M1/E2$ transitions are very intense compared to the $\Delta I=2$ $E2$ crossover transitions. The ratios of the reduced magnetic-dipole and stretched electric-quadrupole transition probabilities were obtained according to the expression

$$\frac{B(M1;I\rightarrow I-1)}{B(E2;I\rightarrow I-2)} = 0.6968\,\frac{E_\gamma^5(I\rightarrow I-2)}{\lambda E_\gamma^3(I\rightarrow I-2)}\,\frac{1}{(1+\delta^2)}(\mu_N^2/e^2{\rm b}^2), \quad (3)$$

TABLE I. Information on transitions assigned to ^{115}Sb.

Energy keV[a]	$I_i^\pi \rightarrow I_f^\pi$	Relative intensity[b]	DCO ratio	Multipolarity[c]
157.8	$19/2^- \rightarrow 15/2^-$	28		$E2$
207.4	$21/2^- \rightarrow 19/2^-$	72		$M1/E2$
214.1	$25/2^+ \rightarrow 23/2^-$	46		$E1$
247.3	$(23/2)^- \rightarrow (21/2)^-$	12	e	$M1/E2$
279.2	$19/2^- \rightarrow 15/2^-$	62		$E2$
319.4	$(25/2)^- \rightarrow (23/2)^-$	4	e	$M1/E2$
322.3	$15/2^- \rightarrow 13/2^-$	< 2	e	$M1/E2$
337.4	$13/2^+ \rightarrow 11/2^+$	58	0.66(8)	$M1/E2$
359.5	$29/2^+ \rightarrow 27/2^+$	31	0.73(10)	$M1/E2$
364.8	$15/2^+ \rightarrow 13/2^+$	52	0.73(8)	$M1/E2$
374.3[d]	$11/2^+ \rightarrow 9/2^+$	76	0.73(7)	$M1/E2$
	$27/2^+ \rightarrow 25/2^+$			
380.6	$17/2^+ \rightarrow 15/2^+$	52	0.61(7)	$M1/E2$
	$(27/2)^- \rightarrow (25/2)^-$			
390.6[d]	$25/2^+ \rightarrow 23/2^+$	51	0.38(5)	$M1/E2$
	$31/1^+ \rightarrow 29/2^+$			
393.6	$33/2^+ \rightarrow 31/2^+$	12	0.38(8)	$M1/E2$
402.2	$35/2^+ \rightarrow 33/2^+$	6	e	$M1/E2$
407.8	$(29/2)^- \rightarrow (27/2)^-$	3	e	$M1/E2$
416.9	$19/2^+ \rightarrow 17/2^+$	34	0.67(11)	$M1/E2$
419.5		13		
427.4[d]	$11/2^+ \rightarrow 9/2^+$	40	0.83(15)	$M1/E2$
	$23/2^+ \rightarrow 21/2^+$			$M1/E2$
434.7	$(31/2)^- \rightarrow (29/2)^-$	< 2	e	$M1/E2$
436.9	$21/2^+ \rightarrow 19/2^+$	31	0.56(8)	$M1/E2$
441.4	$23/2^- \rightarrow 21/2^-$	50		$M1/E2$
443.3	$19/2^- \rightarrow 15/2^-$	54	0.92(8)	$E2$
454.1	$37/2^+ \rightarrow 35/2^+$	5	e	$M1/E2$
461.3	$(33/2)^- \rightarrow (31/2)^-$	< 2	e	$M1/E2$
483.3	$27/2^- \rightarrow 23/2^-$	5	0.97(17)	$E2$
540.4	$21/2^- \rightarrow (21/2)^-$	10	e	$M1/E2$
576.4	$11/2^- \rightarrow 7/2^+$	13		$M2$
581.5	$23/2^- \rightarrow 19/2^-$	52	1.11(7)	$E2$
597.8	$31/2^- \rightarrow 27/2^-$	12	1.03(14)	$E2$
602.6	$9/2^+ \rightarrow 7/2^+$	4		$M1/E2$
623.4		7		
656.8	$9/2^+ \rightarrow 7/2^+$	16		$M1/E2$
685.5	$(27/2)^+ \rightarrow (25/2)^+$	8		$(M1/E2)$
699.5	$(27/2)^- \rightarrow (23/2)^-$	< 2	e	$(E2)$
702.1	$15/2^+ \rightarrow 11/2^+$	7	e	$E2$
712.2	$13/2^+ \rightarrow 9/2^+$	8	e	$E2$
716.4	$35/2^- \rightarrow 31/2^-$	14	1.06(14)	$E2$
720.3	$27/2^- \rightarrow 23/2^-$	31	1.01(8)	$E2$
723.6	$7/2^+ \rightarrow 5/2^+$	28	0.49(4)	$M1/E2$
734.4	$29/2^+ \rightarrow 25/2^+$	5	e	$E2$
745.8	$17/2^+ \rightarrow 13/2^+$	15	1.12(37)	$E2$
750.2	$31/2^+ \rightarrow 27/2^+$	7	e	$E2$
765.5	$27/2^+ \rightarrow 23/2^+$	14	e	$E2$
784.8	$33/2^+ \rightarrow 29/2^+$	4	e	$E2$
788.6	$(29/2)^- \rightarrow (25/2)^-$	<2	e	$(E2)$
797.8[d]	$19/2^+ \rightarrow 15/2^+$	15	e	$E2$
	$35/2^+ \rightarrow 31/2^+$			
818.1	$25/2^+ \rightarrow 21/2^+$	11	e	$E2$
823.3	$39/2^- \rightarrow 35/2^-$	6	0.94(23)	$E2$

TABLE I. (*Continued*.)

Energy keV[a]	$I_i^\pi \rightarrow I_f^\pi$	Relative intensity[b]	DCO ratio	Multipolarity[c]
843.5	$(31/2)^- \rightarrow (27/2)^-$	< 2	e	$E2$
846.9	$31/2^- \rightarrow 27/2^-$	23	1.02(13)	$E2$
854.5	$21/2^+ \rightarrow 17/2^+$	11	0.82(27)	$E2$
856.1	$37/2^+ \rightarrow 33/2^+$	< 2	e	$E2$
864.6	$23/2^+ \rightarrow 19/2^+$	10	e	$E2$
887.4	$31/2^- \rightarrow 27/2^-$	8	0.91(3)	$E2$
890.4	$(33/2)^- \rightarrow (29/2)^-$	< 2	e	$(E2)$
932.2	$43/2^- \rightarrow 39/2^-$	3	1.01(2)	$E2$
959.6	$35/2^- \rightarrow 31/2^-$	11	0.98(21)	$E2$
971.2		3	e	
986.6		5	e	
1015.6	$13/2^- \rightarrow 11/2^-$	20		$(M1/E2)$
1046.6	$47/2^- \rightarrow 43/2^-$	< 3	e	$E2$
1051.4[d]	$39/2^- \rightarrow 35/2^-$	14	1.00(02)	$E2$
1051.6				
1073.3		23		
1098.5	$7/2^+ \rightarrow 5/2^+$	3	e	$M1/E2$
1136(1)	$39/2^- \rightarrow 43/2^-$	< 2	e	$E2$
1154.8(5)	$51/2^- \rightarrow 47/2^-$	< 2	e	$E2$
1216.7	$15/2^- \rightarrow 11/2^-$	100	1.04(8)	$E2$
1300.2	$11/2^- \rightarrow 5/2^+$	211		$E3$
1326.8	$9/2^+ \rightarrow 5/2^+$	15		$E2$
1338.2	$15/2^- \rightarrow 11/2^-$	17		$E2$
1380.5	$9/2^+ \rightarrow 5/2^+$	29		$E2$
1492.8	$27/2^- \rightarrow 23/2^-$	8	0.9(2)	$E2$
1590.1	$23/2^- \rightarrow 19/2^-$	< 2	e	$(E2)$
1754.8(5)	$23/2^- \rightarrow 19/2^-$	4	e	$(E2)$

[a]The errors are given on last digit. Transition energies accurate to within ± 0.3 keV, unless otherwise quoted.
[b]Intensities are normalized to 100 for the 1217 keV transition. The error in intensities is less than 5%.
[d]Intensity quoted for the doublet.
[c]Multipolarity for known transitions adopted from previous works.
[e]Transition too weak for the DCO analysis.

where

$$\lambda = \frac{T_\gamma(I \rightarrow I-2)}{T_\gamma(I \rightarrow I-1)}.$$

The earlier work of Shroy *et al.* [8] reports a small positive mixing ratio (~ 0.2) for the $\Delta I = 1$ $M1/E2$ transitions and its influence on the preceding expression is not significant. Thus, the experimental $B(M1;I \rightarrow I-1)/B(E2;I \rightarrow I-2)$ values have been obtained by neglecting the mixing ratio.

TABLE II. $A(2)$ coefficients of some γ rays assigned to ^{115}Sb.

E_γ (keV)	$A(2)/A(0)$
443.3	$0.27(\pm 0.012)$
581.5	$0.25(\pm 0.014)$
720.3	$0.29(\pm 0.010)$
1216.7	$0.28(\pm 0.015)$
1492.8	$0.52(\pm 0.15)$

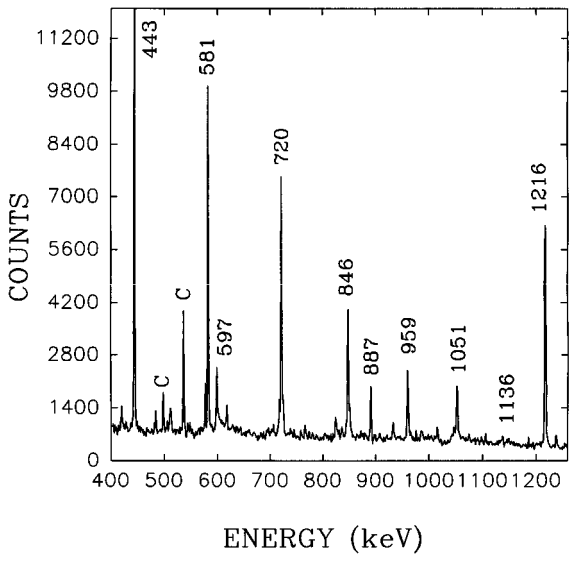

FIG. 2. Sum of γ-ray spectra gated by the members of the band 1. Gating transitions are at 443, 581, 720, 846, 959, and 1051 keV. Prominent peaks labeled with a *C* are contaminants.

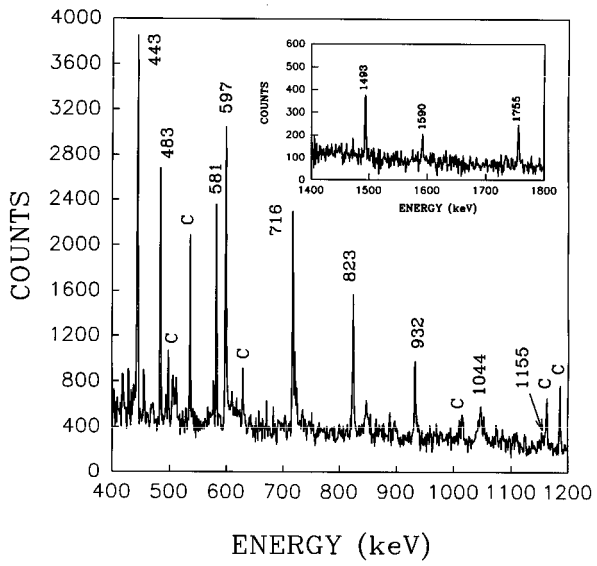

FIG. 3. Sum of γ-ray spectra gated by the members of the band 2. Gating transitions are at 597, 716, 823, 932, and 1044 keV. The inset shows the linking transitions. Prominent peaks labeled with a *C* are contaminants.

E. Band 4

Band 4 is a weakly populated strongly coupled band ($\Delta I=1$) similar in spacings to band 3, and has been found to feed the $I^{\pi}=21/2^{-}$ spherical state through the known 540 keV γ transition. The spin parity assignments for this band are tentative and is based on the systematics of the odd Sb isotopes in which negative parity strongly coupled bands have been observed [4,6]. A positive parity assignment for this band is ruled out as the measurement of internal conversion coefficients of the 247 keV and 540 keV γ transitions by Bron *et al.* [16] supports the $M1/E2$ assignment. This band begins at spin $(23/2^{-})$ and extends to $(33/2^{-})\hbar$. Apart from the relatively strong $\Delta I=1$ transitions, a few weak crossover $E2$ transitions have been observed.

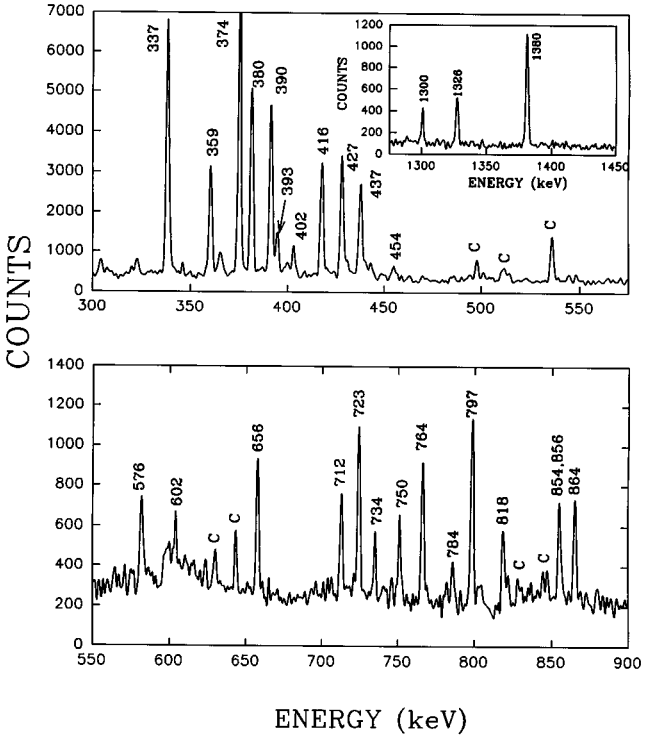

FIG. 4. Gated spectrum of band 3 gated by the 364 keV transition. Prominent peaks labeled with a *C* are contaminants.

TABLE III. The calculated equilibrium deformations.

Neutrons	$[404]9/2^{+}$		$[431]1/2^{+}$		$[550]1/2^{-}$	
	β_2	β_4	β_2	β_4	β_2	β_4
58	0.165	0.030	0.111	0.018	0.149	0.056
60	0.187	0.032	0.116	0.010	0.248	0.082
62	0.196	0.030	0.115	0.001	0.292	0.018
64	0.200	0.022	0.109	0.000	0.264	0.053
66	0.197	0.010	0.094	-0.002	0.257	0.035
68	0.190	0.001	0.083	0.001	0.242	0.020
70	0.175	-0.004	0.070	0.002	0.074	0.018
72	0.149	-0.001	0.058	0.003	0.061	0.017

III. POTENTIAL ENERGY SURFACE CALCULATIONS

In order to pin down the deformations of the various intrinsic configurations in Sb isotopes, the potential energy surface was minimized with the last particle constrained to occupy one of the Nilsson states close to the Fermi surface. This method is based on the Nilsson-Strutinsky shell correction method [19]. The total energy in this method is a sum of the macroscopic and the microscopic parts. The macroscopic part which is a smooth function of the particle number is obtained from a finite range liquid drop model [20]. The microscopic part which is the shell correction term to the liquid drop energy has two components. One component is the shell correction term with no pairing interaction term and is calculated in the present work using the Woods-Saxon potential with the universal parametrization [21,22]. The pairing term is assumed to be of the usual monopole form and has been solved using the BCS approximation. The number fluctuation inherent in the BCS method is partially remedied with the Lipkin-Nogami correction term [23].

The total energy is a functional of the deformation parameters β_2, β_3, and β_4. In the present work we have carried out the minimization of the total energy with respect to β_2 and β_4 only, as the nuclei under investigation are not expected have octupole deformation. The calculations have been performed for a series of Sb isotopes ranging from $A=109$ to 121. The energy minimization has been carried out with the valence proton constrained to occupy the Nilsson configurations $[404]9/2^{+}$, $[431]1/2^{+}$, and $[500]1/2^{-}$. For low deformations, the last proton occupies the $[431]1/2^{+}$ orbital for odd Sb isotopes. However, with increasing deformation there is a crossing between the $[404]9/2^{+}$ and $[431]1/2^{+}$ Nilsson states and the last proton occupies the $[404]9/2^{+}$ state. Further increase in the deformation makes the downsloping $[550]1/2^{-}$ state originating from the intruder subshell $1h_{11/2}$ as the favored configuration. Rotational bands have been observed in this region based on all these three intrinsic configurations [4]. The calculated deformations for the three intrinsic configurations are presented in Table III.

The calculated deformation for the odd proton in the Nils-

son state $[404]9/2^+$ is almost constant for all the Sb isotopes. The earlier calculations of Heyde *et al.* [24] predict smaller equilibrium deformation values compared to the present calculations. Our results for this configuration agree well with the recent calculations of LaFosse *et al.* [6]. When the odd proton occupies the $[431]1/2^+$ state the deformation is nearly constant for $N=58-64$ and decreases for $N>64$. The odd proton in the $[550]1/2^-$ state results in the deformation peaking at $N=62$. The Woods-Saxon calculation shows a peaking at $N=62$, whereas the experimental data show peaking at the midshell region. This feature has recently been pointed out by Raman *et al.* [25] in their study of the ground state deformations of Xe isotopes. Because of identical boson number, the $4p$ bands in Xe nuclei are known to be similar to the $2p$-$2h$ bands in the even-even Sn nuclei [14]. Thus, the deformations of the $\pi h_{11/2}$ decoupled bands in odd Sb nuclei are expected to have similar trends.

IV. DISCUSSION

The band structures observed in odd mass nuclei [26] can be broadly grouped into two categories. In one group, when the odd particle occupies a high-Ω state a $\Delta I=1$ rotational band is observed. In the other group, when the odd particle occupies the low-Ω state of a high-j orbital, the odd particle motion is effectively decoupled from the core by Coriolis force. The resulting band structure has spacings similar to its even-even core. In the present study, both these bands have been observed and are discussed in the following subsections. The configuration assignments are based on (a) the known previous work, (b) comparision with neighboring nuclei in this mass region, and (c) theoretical calculations.

A. $\pi h_{11/2}$ intruder bands

The negative parity assigned to band 1 suggests the occupation of the $h_{11/2}$ orbital by the valence proton. The $\pi h_{11/2}$ orbital alone does not have the deformation driving ability to deform the spherical ^{114}Sn core, as is obvious from the fact that no rotational bands are built on the spherical $11/2^-$ state at 1300 keV. The observed band is interpreted as due to the coupling of this odd proton in $h_{11/2}$ orbital to the known deformed $2p$-$2h$ state of ^{114}Sn [14].

Decoupled bands have been observed in this mass region due to the odd proton occupying the low-Ω state of the $h_{11/2}$ intruder orbital; in addition, in ^{117}Sb [4] decoupled bands based on the $\pi g_{7/2}$ and $\pi d_{5/2}$ orbitals have also been reported. The energy spacings of band 1 are close to that of the ^{114}Sn $2p$-$2h$ band and are similar to the $\pi h_{11/2}$ decoupled bands reported in ^{111,113,117}Sb. Hence, band 1 is interpreted to be a decoupled band based on the odd proton in $\pi h_{11/2}$ orbital coupled to the deformed $2p$-$2h$ state of ^{114}Sn. The observation of such bands near the beginning of a shell implies that the band has a prolate deformation. For oblate deformations, the high-Ω orbital is close to the Fermi surface and its occupation would have resulted in a $\Delta I=1$ rotational band and not a decoupled band.

In band 1, only the favored signature branch of the $\pi h_{11/2}$ band has been observed. Occupation of the low-Ω state of the $h_{11/2}$ intruder orbital results in a large signature splitting and the unfavored signature partner is usually not observed. When the proton Fermi surface is well above the low-Ω states of the $h_{11/2}$ intruder orbital, as in odd mass Cs nuclei, both signatures of the $\pi h_{11/2}$ band are observed [27]. In band 1, we do not see the band down to its bandhead spin of $11/2^-$ but instead to a spin of $15/2^-$. All the known $\pi h_{11/2}$ bands in the ^{111,113,117}Sb nuclei [6,2,4] do not extend down to the bandhead spin of $11/2^-$, and the $2p$-$2h$ bands in the ^{108,110,112}Sn nuclei [11,3,28], also do not extend to 0^+. This is due to appreciable mixing of the low spin members of the bands with the spherical states and the preferential decay with a high energy quadrupole transition compared to the in-band transition which would be of a much lower transition energy.

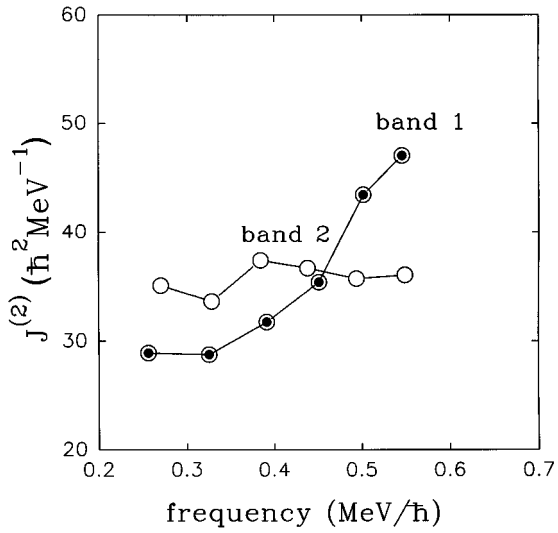

FIG. 5. The dynamic moment of inertia, $J^{(2)}$, plot for band 1 and band 2.

Figure 5 depicts the dynamic moment of inertia ($J^{(2)}$) plot for both band 1 and band 2. Band 1 shows an upbend in the $J^{(2)}$ plot which signifies the onset of alignment. In this data set we do not populate states with high enough spins to see it to the point of complete alignment. Compared to the dynamic moment of inertia of band 1, the $J^{(2)}$ plot of band 2 is relatively flat. Also the two bands have a relative alignment of approximately $4\hbar$ at low frequencies. The aligned angular momentum plot of band 1 and band 2 is shown in Fig. 6. For comparision the aligned angular momentum plot of band 3 and the $2p$-$2h$ band in ^{114}Sn is also displayed.

Cranked shell model calculations employing a universal Woods-Saxon single-particle potential and monopole pairing [21] have been performed at the deformation value predicted by the potential energy surface calculations (Table III). The alignment due to $h_{11/2}$ neutrons is predicted to occur at $\hbar\omega \sim 0.34$ MeV. The $\pi h_{11/2}$ BC, $\pi g_{7/2}$, and $\nu g_{7/2}$ crossings are predicted to occur at a much higher frequency (>0.6 MeV/$\hbar$). The experimental dynamic moment of inertia plot of band 1 in Fig. 5 shows a gradual upbend at a frequency greater than 0.5 MeV/$\hbar$. It is to be noted here that in the $2p$-$2h$ band of ^{114}Sn the $\nu h_{11/2}$ alignment occurs at a frequency ~ 0.4 MeV/$\hbar$ [14]. The $2p$-$2h$ bands in even-even ^{110,112,114}Sn nuclei display sharp crossings [6,2,14], whereas this band crossing occurs at a much higher frequency and with a large interaction strength in the observed $\pi h_{11/2}$ bands

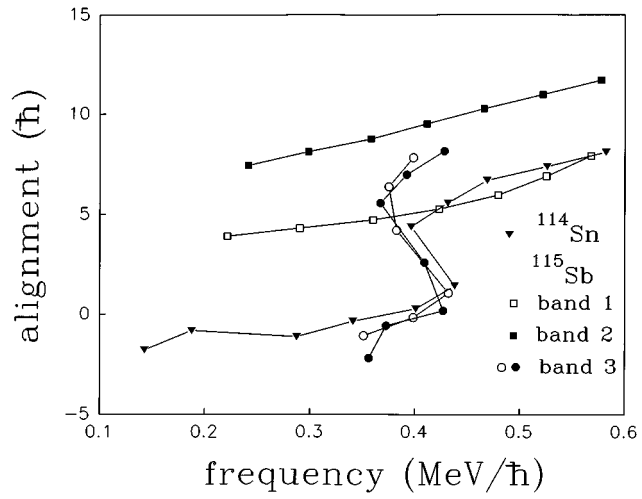

FIG. 6. Aligned angular momentum plot of band 1, band 2, both signatures of band 3, and the $2p$-$2h$ band in ^{114}Sn. The Harris parameters are $J_0=23$ MeV$^{-1}\hbar^2$ and $J_1=0$ MeV$^{-3}\hbar^4$, and are adopted from the neighboring nucleus ^{113}Sb [2].

in odd Sb isotopes. The delay in the $\nu h_{11/2}$ alignment for these bands has been explained by Janzen *et al.* [2,30] as a signature of a high-j residual neutron-proton interaction between the odd proton and the aligning neutrons occupying the same $h_{11/2}$ subshell. A similar effect probably persists in band 1 of ^{115}Sb.

The interesting feature of band 2, which has been assigned negative parity, is the observation of direct decays (quadrupole transitions) into band 1 and to the isomeric state at $I^\pi=19/2^-$. The transition energies in this band are found to be roughly similar to that of band 1. Since band 1 is deduced to have a $11/2^-$ bandhead, we infer that the bandhead spin of band 2 is $19/2^-$ (again band 2 does not follow down to its bandhead spin due to the competing high energy γ transitions). Experimentally we have not observed a signature partner of band 2. At low frequencies a relative alignment of $4\hbar$ exists between band 1 and band 2.

The excited intruder band in ^{115}Sb (band 2), *extending to such low frequencies*, is unique among the known bands in odd mass Sb isotopes and is the first such observation in this mass region. The known excited intruder bands in ^{109,111}Sb [5,6] (i) do not extend to such low frequencies, (ii) different bands in the same nucleus do not have near identical transition energies, and (iii) the transitions linking these bands to the low lying levels were not found. The configuration assignments of such bands in ^{109,111}Sb was supported by Nilsson-Strutinsky cranking calculations (using a harmonic oscillator potential, without pairing) [12,13], which give a good description of the observed band terminating features.

We try to assign the configuration for this band by presenting arguments based on the Nilsson diagram, for, e.g., the one in [11] is appropriate for this mass region. A similar analysis was presented for the possible quasiparticle configurations of the excited intruder bands in ^{111}Sb [6]. The configurations giving rise to negative parity involve either an odd number of (i) neutrons or (ii) protons in the $h_{11/2}$ orbital, coupled to excitations of the Sn $2p$-$2h$ core. The Sn $2p$-$2h$ state has the configuration $(\pi g_{7/2})^2\otimes(\pi g_{9/2})^{-2}{}_{J=0}$ [3]. The first scenario can be accounted for by excitation of neutrons in $(d_{5/2}\otimes g_{7/2})$ orbitals to the $h_{11/2}$ orbital. If one assumes similar deformations for band 1 and band 2, then at the calculated deformation (Table III), this quasiparticle configuration will result in a significant K value for band 2 and a signature partner should have been observed. Alternatively, configurations involving three protons in $h_{11/2}$ orbital are expected to have a large deformation, as the protons would occupy the low-Ω states of the $h_{11/2}$ orbital, all of which are deformation driving. This is likely to affect the moment of inertia and may not preserve the near similarity between band 1 and band 2. The known such bands which have been interpreted to be based on configurations involving $(\pi h_{11/2})^2$ do have a larger moment of inertia and this is best exemplified in ^{113}I [7].

Rotationally aligned protons in the mixed $(d_{5/2}\otimes g_{7/2})$ orbitals coupled to the odd proton in $h_{11/2}$ orbital is another possible configuration for band 2. Such a configuration is yrast according to the cranking calculations at frequencies greater than 0.6 MeV/$\hbar$, which is beyond the observed frequency range in the present data set. Also a $1p$-$1h$ proton excitation of the type $\pi(g_{9/2}^{-1}\otimes h_{11/2})$ will result in a strongly coupled band having a high K value. A strongly coupled band based on such a configuration has been reported in ^{114}Sn [14].

A three-quasiparticle state consisting of a proton in the $d_{5/2}$ orbital coupled to odd number of neutrons in the $h_{11/2}$ orbital is another plausible configuration for band 2. For the considered deformation ($\beta_2\sim0.26$), one of the unpaired neutron would occupy the [413] $5/2^+$ normal parity Nilsson orbital, which is close to the neutron Fermi surface and the other neutron would occupy the [541] $5/2^-$ orbital. This configuration could account for the relative flatness in the $J^{(2)}$ plot, because the first $\nu h_{11/2}$ alignment would be blocked. If one inspects the Nilsson diagram, the normal parity [413] $5/2^+$ orbital has a high K value and will not have appreciable signature splitting. In the neighboring odd-odd ^{114}Sb nucleus [29] bands based on both the signature partners of the odd neutron occupying the [413] $5/2^+$ $\nu g_{7/2}$ orbital coupled to the $\pi h_{11/2}$ orbital have been observed.

Thus, all the above configurations considered do not account for the experimentally observed features of (i) relative spin alignment of $4\hbar$ at low frequencies between band 1 and band 2, (ii) the near similarity of the transition energies in the two bands, and (iii) the nonobservation of the signature partner of band 2.

Following a suggestion due to [31], we extract the relative transition strengths

$$R(B(E2))=\frac{B(E2)_{I^\pi=27/2^-\text{ band }2\rightarrow I^\pi=23/2^-\text{ band }1}}{B(E2)_{I^\pi=27/2^-\text{ band }2\rightarrow I^\pi=23/2^-\text{ band }2}} \quad (4)$$

from the experimental data. This value was deduced using the efficiency corrected intensities of the 483 and 1493 keV γ transitions from the 597 keV gate of band 2. The value of $R(B(E2))$ is deduced to be $0.000\,52\pm0.000\,02$. Thus, the two bands have very little mixing at the bandheads. Since the relative spin alignment between the two bands is $4\hbar$ at low spins, any collective $E2$ transitions between the two bands will be hindered. At $I^\pi=39/2^-$ energy levels of band 1 and band 2 are 53 keV apart, implying that the interaction strength is less than or equal to 27 keV. If they were to

interact at these spin values, one would have observed interband $E2$ transitions. However, within the observational limit, we have not seen any such candidate γ transitions. Hence, it appears that the two bands are nearly diabatic. A two-band-mixing analysis of the levels near the bandheads and the $39/2^-$ states has been carried out. An upper limit of the intensity of the unobserved γ transitions has been estimated from the background in the coincidence spectra. The expressions related to the interaction strength have been taken from Ref. [32] [in which they assume identical $B(E2)$ strengths in the two bands and the nondiagonal matrix elements to be zero]. The deduced interaction matrix element between band 1 and band 2 at $I^\pi=27/2^-$ is 74(6) keV and at $I^\pi=39/2^-$ it is 13(2) keV.

The only *alignable* orbitals in the observed frequency range are neutrons in the $h_{11/2}$ orbital. Cranked shell model calculations predict alignments due to other quasiparticles at a much higher frequency and can therefore be ruled out. Thus the observed spin alignment of four units is probably due to the alignment of $h_{11/2}$ neutrons. Band 2 is yrast beyond spin $43/2^-$ (Fig. 1) and it crosses band 1 at a frequency $\sim$0.41 MeV/$\hbar$. Therefore, band 2 has been interpreted as a structure based on aligned $h_{11/2}$ neutrons. As the two bands have very small interaction strength, band 2 is seen down to very low spin values. The observed γ transitions at 483, 597, and 716 keV are interpreted to be members of the yrare extension of this aligned configuration. The near similarity of the transition energies in band 1 and band 2 implies a spectator role of the aligned $h_{11/2}$ neutrons with a constant alignment of $4\hbar$. Similar crossings have been observed in the rare earth nuclei [33]; however, the yrare extension of the aligned band is not seen to very low spin values.

The nucleus in which nearly diabatic bands have been observed is ^{187}Au, wherein the two $9/2^+$ based bands [34] differ in the occupancy of the intruder $h_{9/2}$ orbital with a small difference in deformation. The experimental data in ^{187}Au has been interpreted within the framework of particle rotor model and the potential energy surface calculations. Unlike the above case, we have interpreted that the diabaticity of the bands 1 and 2 in ^{115}Sb is based on the difference of their aligned angular momenta ($4\hbar$). It is to be noted that in ^{114}Sn the gain in alignment due to $h_{11/2}$ neutrons is about $6\hbar$, whereas in ^{115}Sb it is only $4\hbar$. Further studies to measure the quadrupole moments of the two bands are particularly important to infer the occupancy of neutrons in the $h_{11/2}$ orbital in band 1 and band 2.

B. Strongly coupled bands

The earlier work of Bron *et al.* [16] and Shroy *et al.* [8] has firmly established the rotational character of the $K=9/2^+$ based ($\Delta I=1$) bands in odd mass Sb isotopes. These bands do not show any appreciable signature splitting which is a characteristic of a high-K band. Based on the mixing ratio measurement for the $I\rightarrow I-1$ transitions [$\delta(E2/M1)>0$], it was argued that these bands have a prolate deformation. These $9/2^+$ based bands arise due to the excitation of a $1g_{9/2}$ proton across the $Z=50$ closed shell. The potential energy surface calculations by Heyde *et al.* [24] for Sb isotopes indeed do predict a deformed minima due to a proton hole in the $[404]9/2^+$ orbital.

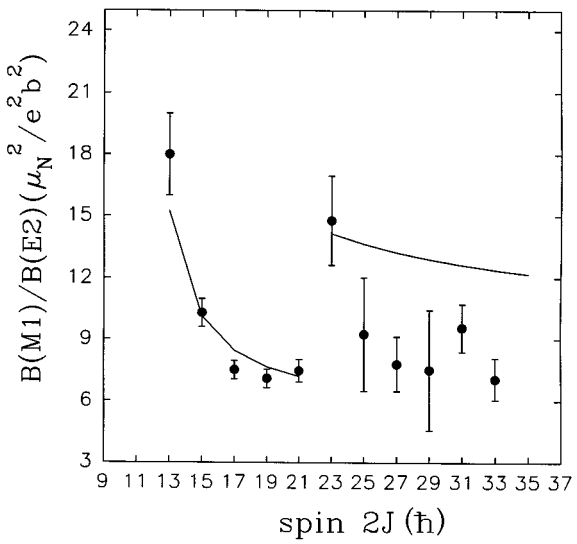

FIG. 7. Experimental $B(M1;I\rightarrow I-1)/B(E2;I\rightarrow I-2)$ ratios of reduced transition probabilities for band 3 are shown with error bars, under the assumption that the multipole mixing ratio is negligible. Geometric model predictions assuming the $(\pi g_{9/2})^{-1}$ (below $21/2\hbar$) and $(\pi g_{9/2})^{-1}\otimes(\nu h_{11/2})^2$ configurations (above $21/2\hbar$) are shown with solid lines. The input values to the Dönau-Frauendorf formula are $g_R=0.44$, $g_p=1.27$, $g_n=-0.21$, and $Q_0=2.63$ e b.

In the present study, we report an extension of the earlier work from $I^\pi=23/2^+$ to $I^\pi=37/2^+$ and also the first clear observation of a backbend for such bands in the odd mass Sb isotopes. Both signatures of band 3 undergo large alignments near the $23/2^+$ state, as depicted in Fig. 6. The crossing occurs near $\hbar\omega=0.40$ MeV, as expected for the $\nu(h_{11/2})^2$ alignment. The gain in alignment of approximately $6\hbar$ is consistent with the predicted quasineutron alignment. The aligned angular momentum plot for the $2p$-$2h$ band in ^{114}Sn is also shown in Fig. 6. The first alignment due to $h_{11/2}$ neutrons in ^{114}Sn has been accounted for by the spin-projected Hartree-Bogoliubov calculations [35]. In the lighter isotopes of Sb, specifically in ^{109,111}Sb, these bands have not been observed down to the bandhead spin of $9/2^+$; instead, they decay out at higher spins [$21/2^+$ in ^{111}Sb [6] and $(19/2)^+$ in ^{109}Sb [5]] to several low lying states. This feature has been inferred as due to decreased deformation and a broader potential minimum, allowing an admixture of the vibrational-like levels to the rotational states [6]. At higher spins, the band is well defined and is thought to be built on aligned $h_{11/2}$ neutrons. In ^{113}Sb [2] the observed alignment is not complete and an upbend occurs at a frequency $\sim$0.40 MeV/$\hbar$. In ^{117,119}Sb [4,8] the bands based on similar configuration do not extend to high enough spins for the $h_{11/2}$ neutron alignment to be observed. This is due to the fact that the light-ion reactions used in those experiments do not populate very high spins, and the $\nu h_{11/2}$ alignment in these isotopes is expected to occur at a higher frequency.

The experimental $B(M1;I\rightarrow I-1)/B(E2;I\rightarrow I-2)$ ratios have been compared with the Dönau-Frauendorf semiclassical expression [36] (Fig. 7), in which the quadrupole moment value has been estimated from the rotational model based on the deformation arrived at from the potential energy surface calculations (Table III). The g factors have been taken from

Ward *et al.* [37] and the g_R value has been deduced from the Z/A scaling. Before the backbend, the experimental ratios start from a high value of $18(\mu_N^2/e^2b^2)$ and decrease with increasing spin. This feature is consistent with the model predictions. The Dönau-Frauendorf expression overestimates the experimental ratios for the aligned $(\pi g_{9/2})^{-1}\otimes(\nu h_{11/2})^2$ configuration. This may be due to (i) different deformation value for the aligned configuration (an increase in deformation will give a better agreement with the experimental value) or (ii) the limitation of the semiclassical expression derived from the one-dimensional cranking (principal axis cranking), which assumes a fixed K value at the bandhead and has limitations in describing high-K bands [38]. According to Frauendorf [39], tilted axis cranking gives a good description for high-K bands in which angular momentum is built by collective rotation as well as by aligning particle spin along the total angular momentum axis. Particle alignment becomes important for weakly deformed nuclei in which the Coriolis force aligns high-K particles along the total spin axis and thus smaller $B(M1)/B(E2)$ are obtained compared to the semiclassical estimate [40].

Extensive calculations by van Isacker *et al.* [41] have been performed for the $K=9/2^+$ based bands in the odd mass Sb isotopes, in which a good agreement of the $M1/E2$ mixing ratio was obtained and a fair agreement with experimental level spacings. In order to get a better agreement with the experimental $13/2^+$-$11/2^+$ level spacing, Shroy *et al.* [8] have performed calculations using the formalism of triaxial rotor [42] and obtained a best fit at $\gamma=20°$. If the $B(E2)$ value is corrected by a $\cos^2(\gamma+30°)$ factor in the Dönau-Frauendorf expression [36], then the estimates will be higher than the present axially symmetric case. In order to describe the present results, after alignment, the particle rotor model calculations need to be extended to involve three quasiparticles which is beyond the scope of the present work.

Band 4 is a weak strongly coupled band feeding the isomeric state at $I^\pi=19/2^-$ through the 540 keV γ transition. The isomer configuration at $I^\pi=19/2^-$ is known from its g factor measurement [8,18] to be the $(\pi g_{7/2})^2\otimes(\pi d_{5/2})\otimes\nu 7^-$ state of ^{114}Sn. Time differential perturbed angular correlation experiments [43] have deduced that the $19/2^-$ isomeric state of ^{115}Sb is deformed and has a quadrupole moment of $Q=52(6)$ fm^2. Band 4 is deduced to be similar in nature to the negative parity strongly coupled band in ^{117}Sb [4], and therefore band 4 has been assigned the configuration $\pi(g_{7/2}^2)\otimes(g_{9/2})^{-1}\otimes 7^-$ state of ^{114}Sn. The first alignment of $h_{11/2}$ neutrons in this band will be blocked as the interpreted configuration has unpaired neutrons in the $h_{11/2}$ orbital and the band is not seen to frequencies high enough to observe other quasiparticle alignments.

V. COMPARISON WITH THE ODD MASS Sb ISOTOPES

It is instructive to compare the emerging features in the odd mass Sb nuclei as neutrons are filled in the $h_{11/2}$ orbital. The bandhead of $\pi(g_{7/2})^2\otimes(g_{9/2})^{-1}$ bands is at the lowest excitation energy in the midshell, in conformity with the known trend. The level spacings of ^{115,117,119}Sb are very similar up to spin $J^\pi=21/2^+$ [8], indicating that the change in deformation over this range is not very large. The calculated deformations of these isotopes (Table 3) for this intrinsic proton configuration are nearly the same.

The observed $\nu h_{11/2}$ backbend in the $\pi(g_{7/2})^2\otimes(g_{9/2})^{-1}$ band in ^{115}Sb, at a frequency $\sim$0.4 MeV/$\hbar$, is sharp, implying a weak interaction between the two crossing bands. The same crossing in the ^{114}Sn $2p$-$2h$ band has similar features [35], whereas in the $\pi h_{11/2}$ intruder band (band 1) of ^{115}Sb a smooth upbend has been observed at a frequency $\sim$0.51 MeV/$\hbar$, clearly indicating that the $h_{11/2}$ neutron alignment is delayed and the smooth upbend implies a larger interaction strength between the two crossing bands. Similar features have been deduced for the $\pi h_{11/2}$ based bands in ^{111,113}Sb, and the extracted interaction strength is larger than the core Sn $2p$-$2h$ bands [6,2]. Janzen *et al.* attribute this feature due to a high-j residual neutron-proton interaction [2,44,30]. Delayed $\nu h_{11/2}$ alignment has also been reported in the $\pi h_{11/2}$ based bands in the neighboring odd proton In, I, and Cs nuclei [45,46,29,27]. Although the mean-field-based calculations describe the existence of the deformed minimum in these isotopes, they do not fully account for the effects due to the residual interactions like those due to n-p [2]. The cranking calculations in Ref. [48] show that explicit inclusion of residual n-p interaction can only account for small shifts in the crossing frequencies. The extended mean field calculations of Satula and Wyss [47] give a good description of the alignment features of the intruder bands in this mass region by including a quadrupole-quadrupole type of pairing. It is to be added here that the recent single-j shell cranking calculations of Frauendorf *et al.* [49] (in which protons and neutrons interact via a δ force) account for the delay in alignment due to the interaction of the odd proton with the $h_{11/2}$ neutrons.

VI. CONCLUSIONS

In summary, the known level scheme of ^{115}Sb has been extended considerably with the placements of two strongly coupled and two new decoupled bands. The configurations of the bands have been made based on the known previous systematics and the total energy calculation. Neutron alignment has been observed in the $K=9/2^+$ strongly coupled band. The same alignment is blocked in the second strongly coupled band which is based on a multiquasiparticle state. In contrast this alignment seems to be delayed in the $\pi h_{11/2}$ based band. An interesting excited intruder band was found whose analog is not found in the neighboring nuclei in this mass region. This band is interpreted to be based on aligned neutrons in the $h_{11/2}$ orbital, which seem to have a spectator role and possibly account for the near similarity of the transition energies of the two intruder bands. It will be interesting to locate such structures in ^{119}Sb and the midshell nucleus ^{117}Sb where bands due to various intrinsic configurations occur at the lowest excitation energy and therefore would be easier to observe experimentally. It is important to establish the existence of the excited intruder bands and their systematic evolution with neutron number.

Note added: Parallel work extending to higher spins has been reported to us by D. R. LaFosse *et al.* [50] using the Chalk River data.

ACKNOWLEDGMENTS

We would like to thank the Pelletron accelerator staff for smooth operation of the machine during the experiment. We are grateful to B. Srinivasan and Dr. M. S. Samant for their help during the experiment. We are very grateful to Prof. Ikuko Hamamoto for stimulating discussions and valuable suggestions. We are thankful to Prof. C. V. K. Baba for suggestions and Dr. J. A. Sheikh for assistance with the potential energy surface calculations. We also thank Professor David Fossan and Dr. Victor Janzen for valuable discussions. We thank D. C. Eprahim and J. Dias for their assistance during the target preparation.

[1] K. Heyde, P. Van Isacker, M. Waroquier, J. L. Wood, and R. A. Meyer, Phys. Rep. **102**, 291 (1983).

[2] V. P. Janzen, H. R. Andrews, B. Haas, D. C. Radford, D. Ward, A. Omar, D. Prévost, M. Sawicki, P. Unrau, J. C. Waddington, T. E. Drake, A. Galindo-Uribarri, and R. Wyss, Phys. Rev. Lett. **70**, 1065 (1993).

[3] J. Bron, W. H. A. Hesselink, A. van Poelgeest, J. J. A. Zalmstra, M. J. Uitzinger, H. Verheul, K. Heyde, M. Waroquier, H. Vincx, and P. van Isacker, Nucl. Phys. **A318**, 335 (1979).

[4] D. R. LaFosse, D. B. Fossan, J. R. Hughes, Y. Liang, P. Vaska, M. P. Waring, and J.-y. Zhang, Phys. Rev. Lett. **69**, 1332 (1992).

[5] V. P. Janzen, D. R. LaFosse, H. Schnare, D. B. Fossan, A. Galindo-Uribarri, J. R. Hughes, S. M. Mullins, E. S. Paul, L. Person, S. Pilotte, D. C. Radford, I. Ragnarsson, P. Vaska, J. C. Waddington, R. Wadsworth, D. Ward, J. Wilson, and R. Wyss, Phys. Rev. Lett. **72**, 1160 (1994); H. Schnare *et al.* (unpublished).

[6] D. R. LaFosse, D. B. Fossan, J. R. Hughes, Y. Liang, H. Schnare, P. Vaska, M. P. Waring, J.-y. Zhang, R. M. Clark, R. Wadsworth, S. A. Forbes, E. S. Paul, V. P. Janzen, A. Galindo-Uribarri, D. C. Radford, D. Ward, S. M. Mullins, D. Prévost, and G. Zwartz, Phys. Rev. C **50**, 1819 (1994).

[7] E. S. Paul, C. W. Beausang, S. A. Forbes, S. J. Gale, A. N. James, P. M. Jones, M. J. Joyce, R. M. Clark, K. Hauschild, I. M. Hilbert, R. Wadsworth, R. A. Cunningham, J. Simpson, T. Davinson, R. D. Page, P. J. Selin, P. J. Woods, D. B. Fossan, D. R. LaFosse, H. Schnare, M. P. Waring, A. Gizon, and J. Gizon, Phys. Rev. C **48**, R490 (1993).

[8] R. E. Shroy, A. K. Gaigalas, G. Schatz, and D. B. Fossan, Phys. Rev. C **19**, 1324 (1979).

[9] A. K. Gaigalas, R. E. Shroy, G. Schatz, and D. B. Fossan, Phys. Rev. Lett. **35**, 555 (1975).

[10] R. Wadsworth, H. R. Andrews, C. W. Beausang, R. M. Clark, D. B. Fossan, A. Galindo-Uribarri, I. M. Hibbert, K. Hauschild, J. R. Hughes, V. P. Janzen, D. R. LaFosse, S. M. Mullins, E. S. Paul, D. C. Radford, H. Schnare, P. Vaska, D. Ward, J. N. Wilson, and I. Ragnarsson, Phys. Rev. C **50**, 483 (1994).

[11] R. Wadsworth, H. R. Andrews, R. M. Clark, D. B. Fossan, A. Galindo-Uribarri, J. R. Hughes, V. P. Janzen, D. R. LaFosse, S. M. Mullins, E. S. Paul, D. C. Radford, H. Schnare, P. Vaska, D. Ward, J. N. Wilson, and R. Wyss, Nucl. Phys **A559**, 461 (1993).

[12] I. Ragnarsson, V. P. Janzen, D. B. Fossan, N. C. Schmeing, and R. Wadsworth, Phys. Rev. Lett. **74**, 3935 (1995).

[13] A. V. Afanasjev and I. Ragnarsson, Nucl. Phys. **A591**, 387 (1995).

[14] M. Schimmer, S. Albers, A. Dewald, A. Gelberg, R. Wirowski, and P. von Brentano, Nucl. Phys. **A539**, 527 (1992).

[15] P. Singh, Ph.D. thesis, University of Bombay, 1993.

[16] J. Bron, W. H. A. Hesselink, H. Bedet, H. Verheul, and G. VandenBerghe, Nucl. Phys. **A279**, 365 (1977).

[17] T. J. Ketel, E. A. Z. M. Verveat, and H. Verheul, Z. Phys. A **285**, 177 (1978).

[18] S. R. Faber, L. E. Young, and F. M. Bernthal, Phys. Rev. C **19**, 720 (1979).

[19] W. Nazarewicz, M. A. Riley, and J. D. Garrett, Nucl. Phys. **A512**, 61 (1990).

[20] P. Möller and J. R. Nix, At. Data Nucl. Data Tables **39**, 213 (1988).

[21] W. Nazarewicz, J. Dudek, R. Bengtsson, and I. Ragnarsson, Nucl. Phys. **A435**, 397 (1985).

[22] S. Ćwiok, J. Dudek, W. Nazarewicz, W. Skalski, and T. Werner, Comput. Phys. Commun. **46**, 379 (1987).

[23] H. C. Pradhan, Y. N. Nogami, and J. Law, Nucl. Phys. **A201**, 357 (1973).

[24] K. Heyde, M. Waroquier, H. Vincx, and P. Van Isacker, Phys. Lett. **64B**, 135 (1976).

[25] S. Raman, J. A. Sheikh, and K. H. Bhatt, Phys. Rev. C **52**, 1380 (1995).

[26] F. S. Stephens, Rev. Mod. Phys. **47**, 43 (1975).

[27] J. R. Hughes, D. B. Fossan, Y. Liang, P. Vaska, and M. P. Waring, Phys. Rev. C **44**, 2390 (1991).

[28] J. L. Wood, K. Heyde, W. Nazarewicz, M. Huyse, and P. Van Duppen, Phys. Rep. **215**, 101 (1992).

[29] E. S. Paul, V. P. Janzen, D. C. Radford, D. Ward, S. M. Mullins, D. B. Fossan, D. R. LaFosse, H. Schnare, H. Timmers, P. Vaska, R. M. Clark, and R. Wadsworth, Phys. Rev. C **50**, 2297 (1994).

[30] V. P. Janzen, Phys. Scr. **T56**, 159 (1995).

[31] I. Hamamoto (private communication).

[32] D. C. Radford, H. R. Andrews, G. C. Ball, D. Horn, D. Ward, F. Banville, S. Flibotte, S. Monaro, S. Pilotte, P. Taras, J. K. Johansson, D. Tucker, J. C. Waddington, M. A. Riley, G. B. Hagemann, and I. Hamamoto, Nucl. Phys. **A545**, 665 (1992).

[33] M. A. Riley, J. Simpson, J. F. Sharpey-Shafer, J. R. Cresswell, H. W. Cranmer-Gordon, P. D. Forsyth, D. Howe, A. H. Nelson, P. J. Nolan, P. J. Smith, N. J. Ward, J. C. Lisle, E. Paul, and P. M. Walker, Nucl. Phys. **A486**, 456 (1988).

[34] D. Rupnik, E. F. Zganjar, J. L. Wood, P. B. Semmes, and W. Nazarewicz, Phys. Rev. C **51**, R2867 (1995).

[35] H. Harada, M. Sugawara, H. Kusakari, H. Shinohara, Y. Ono, K. Furuno, T. Hosoda, M. Adachi, S. Matsuki, and N. Kawamura, Phys. Rev. C **39**, 132 (1989).

[36] F. Dönau and S. Frauendorf, in *Proceedings of the Conference on High Angular Momentum Properties of Nuclei, Oak Ridge, 1982*, edited by N. R. Johnson (Harwood Academic, New York, 1982), p. 143; F. Dönau, Nucl. Phys. **A471**, 469 (1987).

[37] D. Ward, V. P. Janzen, H. R. Andrews, D. C. Radford, G. C. Ball, D. Horn, J. C. Waddington, J. K. Johansson, F. Banville, J. Gascon, S. Monaro, N. Nadon, S. Pilotte, D. Prévost, P. Taras, and R. Wyss, Nucl. Phys. **A529**, 315 (1991).
[38] R. Bengtsson, Nucl. Phys. **A557**, 277c (1993).
[39] S. Frauendorf, Nucl. Phys. **A557**, 259c (1993).
[40] S. Frauendorf (private communication).
[41] P. Van Isacker, M. Waroquier, H. Vincx, and K. Heyde, Nucl. Phys. **A292**, 125 (1977).
[42] J. Meyer-ter-Vehn, Nucl. Phys. **A249**, 111 (1975); Nucl. Phys. **A249**, 141 (1975).
[43] W. Semmler, H.-E. Mahnke, H. Grawe, and R. Sielemann, Z. Phys. A **309**, 349 (1983).
[44] R. Wyss and A. Johnson, in *Proceedings of the International Conference on High Spin Physics and Gamma-Soft Nuclei*, Pittsburgh/Carnegie-Mellon, edited by J. X. Saladin, R. A. Sorensen, and C. M. Vincent (World Scientific, Englewood Cliffs, NJ, 1991), p. 123.
[45] S. M. Mullins, V. P. Janzen, P. Vaska, D. B. Fossan, G. Hackman, D. R. LaFosse, E. S. Paul, D. Prévost, H. Schnare, J. C. Waddington, R. Wadsworth, D. Ward, and M. P. Waring, Phys. Lett. B **318**, 592 (1993).
[46] E. S. Paul, M. P. Waring, R. M. Clark, S. A. Forbes, D. B. Fossan, J. R. Hughes, D. R. LaFosse, Y. Liang, R. Ma, P. Vaska, and R. Wadsworth, Phys. Rev. C **45**, R2537 (1992).
[47] W. Satula and R. Wyss, Phys. Scr. **T56**, 159 (1995).
[48] W. Satula, R. Wyss, and F. Dönau, Nucl. Phys. **A565**, 573 (1993).
[49] S. Frauendorf, in *Proceedings of the Workshop on Gamma-sphere Physics*, Berkeley, 1995 (World Scientific, Singapore, in press); S. Frauendorf and J. A. Sheikh, Phys. Rev. Lett. (submitted).
[50] D. R. LaFosse (private communication).